Global But Not Gonadotrope-Specific Disruption of *Bmal1* Abolishes the Luteinizing Hormone Surge Without Affecting Ovulation

Adrienne Chu, Lei Zhu, Ian D. Blum, Oliver Mai, Alexei Leliavski, Jan Fahrenkrug, Henrik Oster, Ulrich Boehm, and Kai-Florian Storch

Douglas Mental Health University Institute and Department of Psychiatry (A.C., I.D.B., L.Z., K.-F.S.), McGill University, Montreal, Quebec H4H 1R3, Canada; Department of Pharmacology and Toxicology (O.M., U.B.), University of Saarland School of Medicine, D-66421 Homburg, Germany; Department of Clinical Biochemistry (J.F.), Bispebjerg Hospital, University of Copenhagen, DK-2400 Copenhagen NV, Denmark; and Circadian Rhythms Group (A.L., H.O.), University of Lübeck, D-23538 Lübeck, Germany

Although there is evidence for a circadian regulation of the preovulatory LH surge, the contributions of individual tissue clocks to this process remain unclear. We studied female mice deficient in the *Bmal1* gene (*Bmal1*$^{-/-}$), which is essential for circadian clock function, and found that they lack the proestrous LH surge. However, spontaneous ovulation on the day of estrus was unaffected in these animals. *Bmal1*$^{-/-}$ females were also deficient in the proestrous FSH surge, which, like the LH surge, is GnRH-dependent. In the absence of circadian or external timing cues, *Bmal1*$^{-/-}$ females continued to cycle in constant darkness albeit with increased cycle length and time spent in estrus. Because pituitary gonadotropes are the source of circulating LH and FSH, we assessed hypophyseal circadian clock function and found that female pituitaries rhythmically express clock components throughout all cycle stages. To determine the role of the gonadotrope clock in the preovulatory LH and FSH surge process, we generated mice that specifically lack BMAL1 in gonadotropes (GBmal1KO). GBmal1KO females exhibited a modest elevation in both proestrous and baseline LH levels across all estrous stages. BMAL1 elimination from gonadotropes also led to increased variability in estrous cycle length, yet GBmal1KO animals were otherwise reproductively normal. Together our data suggest that the intrinsic clock in gonadotropes is dispensable for LH surge regulation but contributes to estrous cycle robustness. Thus, clocks in the suprachiasmatic nucleus or elsewhere must be involved in the generation of the LH surge, which, surprisingly, is not required for spontaneous ovulation. **(*Endocrinology* 154: 2924–2935, 2013)**

A link between a daily timer and the reproductive axis has already been suggested by early work examining the effect of barbiturate sedation on the expression of the preovulatory LH surge in rats (1). Barbiturate treatment during a critical time window on the afternoon of proestrus acutely suppressed the LH surge and delayed it by exactly 1 day (1). Because barbiturates are short-acting central nervous system depressants, it was postulated that a daily neuronal signal triggers ovulation. Experimental evidence for a key role of the circadian clock in LH surge timing was also provided in ovariectomized (OVX) rodents supplemented with surge-permissive estradiol (E2) levels (2). These animals exhibited a daily LH surge just before lights off, mirroring the timing observed in intact animals during proestrus (3). Importantly, this daily LH rise continued even under conditions of constant darkness (DD) and was stably phase-linked with the circadian clock-controlled rest-activity cycle (4).

In mammals, the master circadian pacemaker resides in the suprachiasmatic nucleus (SCN) located in the anteroventral hypothalamus. The SCN pacemaker is thought to regulate physiological and behavioral rhythms through

ISSN Print 0013-7227 ISSN Online 1945-7170
Printed in U.S.A.

Received January 18, 2013. Accepted May 28, 2013.
First Published Online June 4, 2013

Abbreviations: CRY, cryptochrome protein; COC, cumulus-oophorus complex; CT, circadian time; DD, constant darkness; DI, metestrus; DII, diestrus II; E2, estradiol; GnRHR, GnRH receptor; GRIC, GnRHR-internal ribosome entry site-Cre; KO, knockout; LD, 12-hour light, 12-hour dark; OVX, ovariectomized; PER, period protein; qPCR, quantitative PCR; SCN, suprachiasmatic nucleus; Tom, tdTomato; WT, wild-type; ZT, zeitgeber time.

neurochemical and neurohumoral output pathways directly, or indirectly by coordinating the oscillations of subordinate clocks that are distributed throughout the body axis (5, 6). The circadian clock is cell-autonomous and molecularly characterized by transcriptional-translational feedback loops. At its core, BMAL1 forms a transcription factor dimer with CLOCK or NPAS2, driving expression of the period (*Per*) and cryptochrome (*Cry*) genes via E-box promoter elements. Period proteins (PER) and cryptochrome proteins (CRY) accumulate over time and then enter the nucleus to repress their own transcription. As PER and CRY levels decrease, the cycle begins anew (5, 7).

SCN-lesioned animals are behaviorally arrhythmic and fail to exhibit a coordinated LH surge (8–10). The importance of SCN function in LH surge generation was elegantly corroborated in behaviorally split OVX+E2 hamsters. Upon constant light exposure, these animals show antiphasic molecular oscillations between the 2 SCN hemispheres and concurrently 2 daily antiphasic activity bouts (11). Both activity bouts are preceded by an LH surge, suggesting that the phase of the SCN pacemaker dictates surge timing (12).

Further support for the relevance of the circadian timing system in reproduction has been provided by animals with genetically perturbed clock function. $Clock^{\Delta 19/\Delta 19}$ mice, which show locomotor period lengthening in DD that eventually leads to arrhythmia (13), are subfertile and are unable to produce an LH surge (14, 15). $Bmal1^{-/-}$ mice become instantaneously arrhythmic in DD (ie, they do not exhibit a discernable 24-hour component of locomotor activity under constant conditions) and are infertile (16, 17). Their infertility is thought to be due to impaired corpus luteum steroidogenesis resulting in embryo implantation failure (16).

Circadian clock gene expression and rhythm generation are not restricted to the master SCN pacemaker but are also observed in other tissues including structures of the reproductive axis, raising the possibility that multiple oscillators contribute to reproductive success (18, 19). However, because the circadian rhythm mutants examined for reproductive deficits carry body-wide gene manipulations, the individual contributions of central and peripheral pacemakers remain unclear.

A central player in the reproductive axis are the gonadotrope cells found in the anterior pituitary, which release LH and FSH into the circulation in response to GnRH. Binding of GnRH to its cognate receptor, GnRHR, raises intracellular calcium levels, triggering LH exocytosis from secretory granules, which causes the rapid rise of circulating LH on proestrus (20, 21). The pituitary is known to exhibit circadian rhythms in gene expression at the whole-organ level (22, 23) and cultured gonadotrope cells have been shown to upregulate period gene expression upon GnRH stimulation (24). Furthermore, noncanonical E-box promoter elements have been detected upstream of the *GnRHR* gene. and *Bmal1* knockdown in an immortalized gonadotrope cell line lowers GnRHR transcript levels (25), raising the possibility that an intrinsic clock in gonadotropes directly regulates GnRH signaling. These findings together with the distinct time-of-day dependency of the proestrous LH rise prompted us to postulate that an intrinsic circadian clock in gonadotropes contributes to LH surge regulation and thus timing of ovulation.

To address this hypothesis, we created conditional knockout (KO) mice that lack the essential clock component BMAL1 selectively in pituitary gonadotropes (GBmal1KO) and tested them alongside $Bmal1^{-/-}$ female mice for deficits in LH surge generation and other reproductive functions.

Materials and Methods

Animals

Animals were housed either under a 12-hour light, 12-hour dark (LD) cycle or in DD. Experiments were carried out in accordance with the protocol approved by the McGill University Animal Care Committee. $Bmal1^{-/-}$ (17), *Bmal1-Luc* (26), and *PER2::LUC* (23) mice were on a C57BL/6J genetic background, whereas GBmal1KO mice (this study) were on a mixed (C57BL/6J and 129SvJ) background. Unless stated otherwise, 2- to 4-month-old female mice were used for experiments with littermates serving as experimental controls.

Genomic and quantitative RT-PCR

For assessing tissue specificity of floxed *Bmal1* allele recombination, genomic DNA of selected tissues (see Supplemental Figure 4D, published on The Endocrine Society's Journals Online web site at http://endo.endojournals.org) was extracted by standard methods (27). Multiplex PCR producing a 431-bp (floxed allele) and a 572-bp (recombined allele) DNA fragment was carried out with primers L1 (5′-ACTGGAAGTAACTTTATCAAACTG-3′) and L2 (5′-CTGACCAACTTGCTAACAATTA-3′), which flank the downstream *LoxP* site at the floxed *Bmal1* locus (28), and primer R4 (5′-CTCCTAACTTGGTTTTTGTCTGT-3′), which is located upstream of the upstream *LoxP* site. For quantitative RT-PCR, pituitaries of C57BL/6J females were collected and immediately flash-frozen at 4-hour intervals. Total RNA was extracted with TRIzol reagent according to the manufacturer's instructions (Life Technologies, Burlington, Ontario, Canada). cDNA was synthesized from 1 μg total RNA using random hexamer primers and the High Capacity reverse transcriptase kit (Applied Biosystems, Burlington, Ontario, Canada). The cDNA equivalent of 25 ng total RNA was used per 25 μl quantitative PCR (qPCR) mix (Quanta BioSciences, Gaithersburg, Maryland). SYBR green-based qPCR was carried out on a Real-Time Cycler ABI Prism 7500 (Life Technologies). Relative transcript abundance was calculated using threshold cycle number difference, normalized to *Gapdh* expression. Primer sequences are listed in Supplemental Table 1.

Immunohistochemistry and histology

Mice were anesthetized with ketamine/xylazine and perfused transcardially with 4% paraformaldehyde in 0.1M PBS. Tissues were removed and postfixed for 24 hours, incubated overnight with 30% sucrose in 0.1M PBS, embedded in optimal cutting temperature compound (OCT, Tissue-Tek; Cedarlane, Burlington, Ontario, Canada), and snap-frozen in dry ice/2-methylbutane. The 18-μm cryosections were mounted on SuperFrost Plus glass slides and stored at −80°C until use.

For immunostaining, pituitary sections were incubated in blocking solution (0.01% Triton X-100, 5% donkey serum in PBS) for 1 hour at room temperature, followed by incubation with primary antibody at 4°C overnight. LH and BMAL1 were detected with goat anti-LH (1:1000; Santa Cruz Biotechnology, Santa Cruz, California) and rabbit anti-Bmal1 (1:1000; Novus Biologicals, Oakville, Ontario, Canada) antibodies, respectively. Secondary antibodies were donkey antirabbit Alexa488 and donkey antigoat Alexa568 (1:500; Invitrogen, Burlington, Ontario, Canada).

For detection of PER1 in LH cells, pituitary sections were first subjected to antigen retrieval using a pH 6 retrieval buffer (catalog item S2031; Dako, Copenhagen, Denmark) as described by the manufacturer. The procedure included a 5-minute treatment of the sections submersed in retrieval buffer in a microwave oven (900 W). Sections were then incubated overnight with rabbit PER1 antibodies (code S298–5) (28) diluted 1:5000 together with the goat LH antibodies described above. PER1 was visualized using biotinylated donkey antirabbit antibodies (Jackson ImmunoResearch Laboratories, Hamburg, Germany) in conjunction with biotinylated tyramide (tyramide system amplification; DuPont NEN Life Science Products, Dreieich, Germany) and streptavidin dye light 488 (Jackson ImmunoResearch Laboratories, Germany). For secondary detection of LH, donkey antigoat Alexa 594 antibodies (Invitrogen) were used. For histological examination, ovaries were dissected, fixed in Bouin's solution for 24 hours, and paraffin-embedded according to standard procedures. The 5-μm–thick sections were obtained with a microtome and stained with eosin-hematoxylin.

Luciferase assays

Luminescence recording of Bmal1-Luc *pituitaries*

Extraction and organotypic culture of pituitary tissue was carried out as described previously (29). Briefly, animals were euthanized by cervical dislocation, and the whole pituitary was quickly extracted and submerged in ice-cold Hanks' buffered saline solution before being transferred onto a membrane insert (PICMORG50, Millicell; Millipore, Billerica, Massachusetts) in a 35-mm petri dish with 1 mL recording medium and a final concentration of 0.1mM luciferin (VivoGlo D-Luciferin salts; Promega, St Laurent, Quebec, Canada). Dishes were hermetically sealed using 40-mm round coverslips (size 0; Harvard Apparatus, Holliston, Massachusetts) and transferred into a Lumicycle (Actimetrics, Wilmette, Illinois) to record global tissue bioluminescence for several days. Data were processed with the provided analysis software.

Luminescence imaging of PER2::LUC *pituitaries*

For ex vivo imaging of circadian rhythms in pituitary, we used pituitaries isolated from heterozygous *PER2::LUC* mice. Pituitary was gently removed from sella turcica and cultured at 37°C, 5% CO_2 on a 0.4-μm Millicell-CM PTFE membrane (Millipore, Billerica, Massachusetts) in DMEM (Invitrogen) supplemented with luciferin (0.1mM). Luminescence was imaged with a LV200 imaging system (Olympus, Hamburg, Germany) and analyzed using the Cell^M software (Olympus).

Reproductive phenotyping

Puberty onset and fertility

Animals were weaned at 3 weeks of age and inspected daily for vaginal membrane breech, which was considered to be the first sign of puberty onset in females. To assess fertility, we housed animals in pairs: 1 WT or GBmal1KO female with 1 C57/BL6 male. To verify that mating occurred, females were checked every morning for the presence of a copulation plug. The first day of plug detection was considered to be gestation day 1.

Estrous cycle assessment

Estrous stage was monitored by daily vaginal lavage with 0.1M PBS and subsequent microscopic inspection of the shed cells. Cycle length determination was based on estrous stage recurrence. Acyclicity was calculated as percentage of days spent noncycling per animal. A period was considered noncyclic if a transition through proestrous/estrous stages did not occur for more than 6 days. *Bmal1*$^{-/-}$ animals were cycle-staged for 3 weeks under an LD cycle followed by 3 weeks in DD. Vaginal lavage was carried out under a 15-W red safety light during DD.

Gonadotropin measurement

Blood from *Bmal1*$^{-/-}$ mice was collected on the day of proestrus from the tail vein at 4 consecutive time points (zeitgeber time [ZT] 7, 11, 15, and 19 or ZT 11, 15, 19, and 23). In case of GBmal1KO, blood collection from tail vein was conducted on either 5 or 7 consecutive days 1 hour before lights off (ZT 11). Blood collection did not exceed 50 μL per time point. Blood samples were placed at 4°C overnight, centrifuged at 1000*g* for 10 minutes, and the retrieved serum was stored at −80°C until use. Vaginal lavage was concurrently conducted to assess cyclicity. Mice were 3 to 6 months of age during the time of experiment. The 8-μL serum aliquots were analyzed for LH and FSH content employing xMAP technology (Luminex) that is based on an ELISA-type fluorescence assay involving magnetic beads. Analysis was carried out on a Luminex 200 platform (Luminex, Toronto, Ontario, Canada) using a Milliplex rat pituitary magnetic beads panel as described by the manufacturer (catalog item RPT86K/RPTMAG-86K; Millipore, Mississauga, Ontario, Canada). Assay limit of detection was 4.9 pg/mL for LH and 47.7 pg/mL for FSH, and intra-assay coefficients of variance were <3.3%.

Sex hormone measurement

Blood was collected by cardiac puncture on the day of proestrus at ZT 11 and processed for serum retrieval as described above. 17β-E2 and progesterone serum levels were measured by RIA according to the manufacturer's protocol (catalog item 07–138102 and 07–170102; MP Biomedicals, Solon, Ohio). Limit of detection was 6 pg/mL (17β-E2) and 0.1 ng/mL (progesterone). Intra-assay coefficients of variance were 6.8% (17β-E2) and 8.7% (progesterone).

Ovulation

To examine cumulus-oophorus complexes (COCs) that accumulated in the fallopian ampullae, oviducts were dissected at ZT 21 to 22 on proestrus or ZT 2 to 3 on estrus and placed in 1× PBS. COCs were gently released by rupturing the ampulla epithelium using forceps.

Statistical analysis

Data were analyzed using GraphPad Prism statistical software. Student's *t* test was used to determine the significance of difference between 2 distributions. Multiple groups were compared using 2-way ANOVA followed by Bonferroni post hoc comparison. Results were considered significant at $P < .05$.

Results

Circadian clock gene expression in the female pituitary and gonadotropes

To ascertain that the female pituitary exhibits the properties of a tissue harboring circadian clocks, we first assessed circadian gene expression across the estrous cycle by qPCR. Genes *Bmal1*, *Rev-erbα*, *Cry1*, and *Dbp* were chosen because they represent clock or clock-controlled genes (*Dbp*) that are known to exhibit robust transcriptional oscillations in most tissues harboring circadian clocks. When female mice were maintained under an LD cycle, transcript levels of *Bmal1*, *Rev-erbα*, *Cry1*, and *Dbp* all exhibited a daily rhythm, although these oscillations varied between cycle stages with regard to amplitude and phase (Figure 1A). On diestrus II (DII) and estrus, *Dbp* showed peak levels at around the time of lights off (ZT 9–13), whereas the peak shifted to later hours on proestrus (ZT 17). Phases of peak expression for *Rev-erbα* (ZT 9) and *Bmal1* (ZT 21–1) did not differ between stages (Supplemental Figure 1). However, *Rev-erbα* transcript oscillations showed a reduction in amplitude at proestrus when compared with estrus and DII, as did *Dbp*. The observed differences in clock gene expression on proestrus versus estrus/diestrus suggest that pituitary rhythm generation is influenced by estrous stage, which has been also reported for the uterus and the ovaries (18).

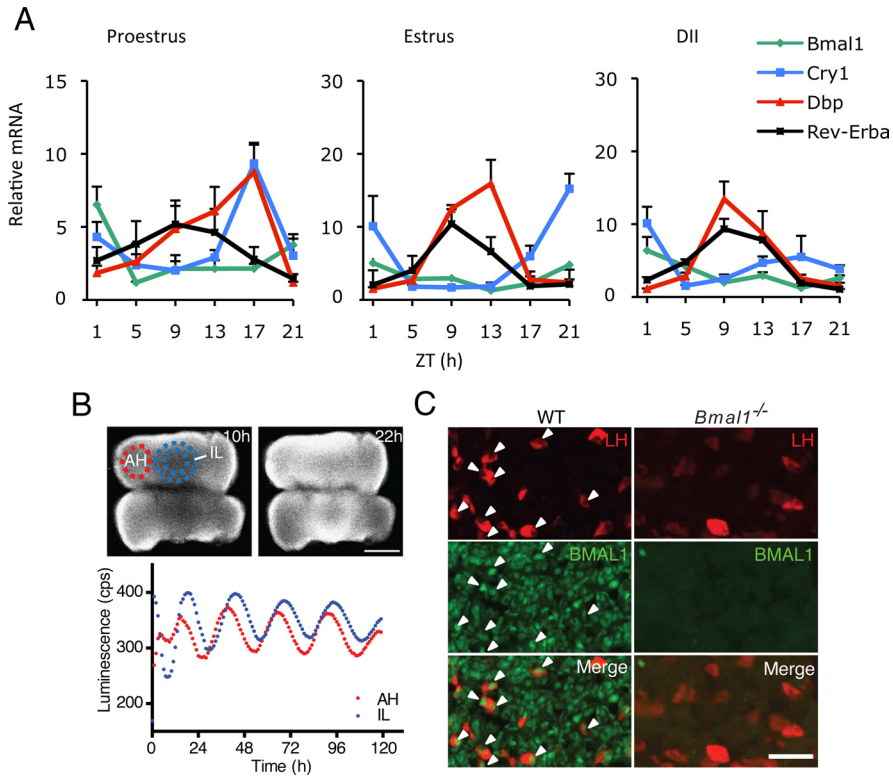

Figure 1. Rhythmic gene expression in female pituitary. A, Daily profiles of *Rev-erbα*, *Cry1*, *Bmal1*, and *Dbp* mRNA abundance in whole mouse pituitary on proestrus, estrus, and diestrus measured by RT-qPCR. Profiles varied according to cycle stage. Relative transcript abundance levels are plotted in arbitrary linear units. Values represent means ± SEM; n = 3 for each time point. B, Bioluminescence imaging of circadian PER2 rhythms in whole female pituitary explants from *PER2::LUC* reporter mice. Top, Image of whole pituitaries at 10 and 22 hours after explantation at ZT 4 to 5. Bottom, Traces of bioluminescence averaged across the pituitary regions demarcated by dotted lines (upper image). Time of explantation is 0 hour. C, Immunohistochemical examination of anterior pituitary sections of WT and *Bmal1*$^{-/-}$ animals using antibodies against BMAL1 and LH. Arrowheads mark BMAL1-positive LH gonadotropes. Scale bar, 50 μm. Abbreviations: AH, adenohypophysis; IL, intermediate lobe.

To further assess clock gene regulation in the female pituitary, we used genetically engineered mice that either carry a luciferase transgene driven by the *Bmal1* promoter (*Bmal1-Luc*) (26) or a knock-in luciferase gene into the *Per2* locus (*PER2::LUC*) (23). Pituitary explants derived from *Bmal1-Luc* mice revealed 24-hour rhythms in bioluminescence persisting over multiple days, confirming that the female pituitary gland harbors a functional clock (Supplemental Figure 1E). Consistent with this, bioluminescence imaging of pituitaries from *PER2::LUC* mice revealed 24-hour rhythms in reporter expression throughout the pituitary, affecting many if not all cell types (Figure 1B and Supplemental Video 1). Interestingly, the average bioluminescence emission rhythm in the anterior pituitary was phase-advanced compared with the intermediate lobe, suggesting differences in intrinsic circadian clock phasing. To test whether gonadotrope cells are also clock cells, we immunostained pituitary sections with antibodies against LH and BMAL1. Although the pituitaries of *Bmal1*$^{-/-}$ mice did not ex-

hibit BMAL1 immunoreactivity (Figure 1C, right column), examination of wild-type (WT) pituitaries revealed that the great majority of LH cells express BMAL1 (Figure 1C, left column). In agreement with previous findings (31), BMAL1 immunoreactivity was largely confined to the nucleus, further corroborating that LH-expressing gonadotropes represent clock cells.

Estrous cycling and gonadotropin regulation in *Bmal1*$^{-/-}$ mice

We next tested *Bmal1*$^{-/-}$ mice for deficits in estrous cycling and gonadotropin regulation. We found that *Bmal1*$^{-/-}$ females spend more time in estrus compared with WT (Figure 2, A and B), a feature that was enhanced under DD conditions (Figure 2C and Supplemental Figure 2, A and B). *Bmal1*$^{-/-}$ females also showed an increase in overall cycle length in DD compared with LD or their WT littermates (Supplemental Figure 2C), and a trend toward acyclicity (Figure 2D).

An increased cycle length in *Bmal1*$^{-/-}$ females has been previously reported (16); however, these authors did not report a bias toward the estrous stage, as has also been also demonstrated for *Clock*$^{\Delta 19/\Delta 19}$ females (14). We next assessed the LH surge in *Bmal1*$^{-/-}$ females, which generally occurs just before the active period (ie, before lights off) on the day of proestrus in nocturnal rodents (1, 3). Blood samples were taken at 4 consecutive time points between ZT 7 and 19 on the days of proestrus and estrus (Figure 3A). Serum analysis revealed the expected proestrous surge around lights off (ZT 11) in WT animals (Figure 3, A and C), whereas *Bmal1*$^{-/-}$ females showed serum LH concentrations at baseline levels throughout all proestrous time points (Figure 3, A and D). An independent second experiment with blood collected between ZT 11 and 23 on the day of proestrus confirmed these results (Supplemental Figure 3A). Throughout estrus, LH remained at baseline levels in *Bmal1*$^{-/-}$ females, as was the case in WT controls (Figure 3A and Supplemental Figure 3B). These data indicate that the LH surge is neither delayed nor shifted to the next day in *Bmal1*$^{-/-}$ animals.

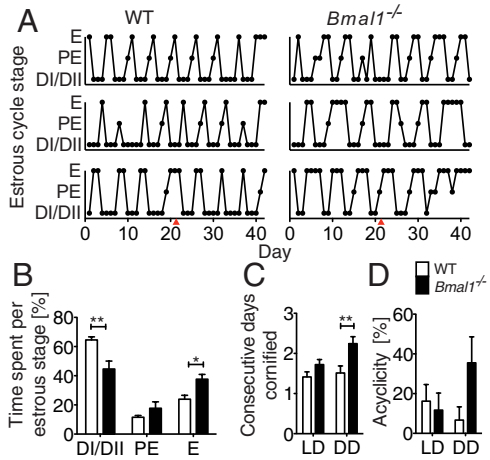

Figure 2. Estrous cycle characteristics of *Bmal1*$^{-/-}$ under LD and DD. A, Representative estrous cycling of individual WT and *Bmal1*$^{-/-}$ females. Transition from LD to DD is indicated on the x-axis (red triangle). B, Percentage of time spent in each estrous stage calculated for the duration of the cycle staging experiment (6 weeks). *Bmal1*$^{-/-}$ females generally spent less time in DI/DII and more time in estrus compared with WT. C, *Bmal1*$^{-/-}$ mice exhibit an increase in consecutive days cornified in DD. D, *Bmal1*$^{-/-}$ also showed a trend toward increased acyclicity in DD, which, however, did not reach significance ($P = .072$). B–D show mean values ± SEM; n = 10 for WT and n = 11 for *Bmal1*$^{-/-}$. By ANOVA: *, $P < .05$; **, $P < .01$. Abbreviations: E, estrus; PE, proestrus.

Although serum FSH concentrations gradually increased on proestrus in WT controls, they remained low in *Bmal1*$^{-/-}$ females (Figure 3B, left). On estrus, however, both groups exhibited a similar gradual decrease from relatively high FSH concentrations at ZT 7 (Figure 3B, right). Due to the blood collection time points we chose, the proestrous/estrous FSH analysis likely revealed the upslope (proestrous data) of the primary FSH surge as well as the downslope (estrous data) of the secondary FSH surge (32, 33). These measurements thus indicate that global elimination of clock function severely blunts or even abolishes the primary FSH surge, whereas the secondary surge remains unaffected. These results are consistent with previous findings suggesting that the primary FSH surge, similar to the LH surge, is triggered by the proestrous GnRH rise, whereas the secondary surge relies on activin signaling that is cyclically inhibited by ovary-borne inhibin (33, 34).

Clock$^{\Delta 19/\Delta 19}$ mice display a similarly blunted LH surge but are nonetheless able to produce offspring (14), raising the possibility that the proestrous LH rise is not essential for ovulation. However, the ability to ovulate has not been tested in cycling, nonmating *Clock*$^{\Delta 19/\Delta 19}$ females. This leaves open the possibility that *Clock*$^{\Delta 19/\Delta 19}$ and *Bmal1*$^{-/-}$ females may act only as induced ovulators, although unable to spontaneously ovulate. In such a case, ovulation would be triggered by copulation, and therefore, mutant females may not need to rely on a circadian clock-driven LH surge (35). To determine whether *Bmal1*$^{-/-}$ females have lost their ability to spontaneously ovulate, we examined the fallopian tubes in *Bmal1*$^{-/-}$ females and their WT littermates in the late hours of the night of proestrus (ZT 21–22). At this time, the COC harboring the ovulated ovum has typically already reached the ampullae, a section of the fallopian tubes that initially accumulate the COCs (36). All inspected *Bmal1*$^{-/-}$ females (5 of 5) and most the WT controls (5 of 7) showed distended ampullae (Figure 3F, arrows) yielding COCs that were morphologically indistinguishable from one another. These findings are consistent with the observation

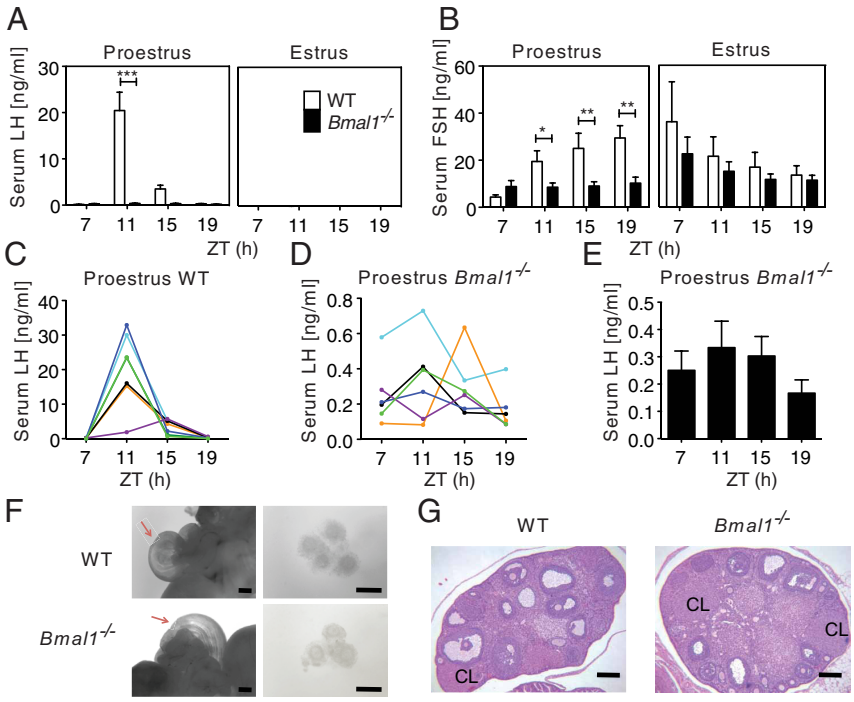

Figure 3. Serum LH/FSH and spontaneous ovulation in *Bmal1*$^{-/-}$ mice. A and B, Proestrous and estrous levels of LH (A) and FSH (B) from ZT 7 to 19, respectively. C and D, Serum LH profiles on proestrus of individual WT (C) and *Bmal1*$^{-/-}$ (D) females. E, Averaged data of D. F, Photographs of representative WT and *Bmal1*$^{-/-}$ fallopian tubes with distended ampullae (arrows) dissected at ZT 22 on proestrus (left) and COCs harvested from ZT 22 ampullae (right) G, Hematoxylin-eosin staining of representative ovary sections from WT and *Bmal1*$^{-/-}$ animals. Scale bars, 100 μm (F) and 200 μm (G). Bar graphs represent mean ± SEM; WT, n = 7; KO, n = 6. By ANOVA: *, $P < .05$; **, $P < .01$; ***, $P < .001$. Abbreviation: CL, corpus luteum.

of corpora lutea in the ovaries of cycling *Bmal1*$^{-/-}$ females (Figure 3G) (37), because corpora lutea are generally thought to result from ovulated follicles. We further confirmed our data on COCs with another cohort of animals that were dissected 5 hours later on the morning of estrus (ZT 2–3). Both genotypes again exhibited distended ampullae and COCs of indistinguishable gross morphology. However, although WT females showed a similar incidence ratio of distended ampullae (5 of 7 animals), fewer *Bmal1*$^{-/-}$ females exhibited such distensions (2 of 5 females) compared with the first inspection 5 hours earlier. On average, *Bmal1*$^{-/-}$ females tended to yield fewer COCs (6.0 ± 0.4) than WT mice (7.3 ± 0.5) (Supplemental Figure 3, C and D); however, this difference did not reach significance ($P = .070$).

Gonadotrope-specific disruption of *Bmal1*

Given the evidence that pituitary gonadotropes represent clock cells and that expression of the essential circadian clock component BMAL1 is required for proestrous LH and FSH surges, we wished to examine the role of local BMAL1 expression in pituitary gonadotropes. To this end, we took advantage of GnRHR-internal ribosome entry site-Cre (GRIC) mice (38), which express Cre recombinase selectively in GnRHR-positive cells. To confirm the suitability of these knock-in mice, we crossed GRIC mice to a tdTomato (Tom)-based Cre reporter line (39) and examined sections of ovary, adrenal gland, pituitary, and SCN from the resulting mice (GRIC-Tom). Ovaries and adrenals lacked specific Tom fluorescence, whereas the pituitary, as expected, exhibited numerous Tom$^+$ cells in the anterior lobe (Supplemental Figure 4B). Consistent with previous findings (40), we observed Tom$^+$ cells scattered in the hypothalamic parenchyma and elsewhere in the brain, but little to no specific Tom fluorescence was detected in the SCN itself (Supplemental Figure 4B). Immunolabeling for LH revealed that LH$^+$ cells invariably expressed Tom, whereas only a few Tom$^+$ LH$^-$ cells could be detected (Supplemental Figure 4C), likely representing FSH$^+$/LH$^-$ gonadotropes (38).

To obtain animals that selectively lack BMAL1 in pituitary gonadotropes (GBmal1KO), we crossed GRIC mice to mice carrying a floxed *Bmal1* allele (Supplemental Figure 4A) (41). GBmal1KO mice were homozygous for the floxed *Bmal1* allele and heterozygous for the *GRIC* allele, whereas WT controls carried only the 2 floxed alleles. To assess recombination of the mutant *Bmal1* alleles in GBmal1KO mice, we analyzed genomic DNA from various peripheral tissues using PCR. Although liver, heart, kidney, ovaries, and pituitaries all showed a PCR product corresponding to the unrecombined floxed *Bmal1* allele, only the pituitary sample additionally produced the band diagnostic for *Bmal1* disruption (Supplemental Figure 4D). Fluorescence microscopic analysis of immunostained pituitary sections then revealed that only 14% ± 3% of the LH-positive gonadotropes coexpressed BMAL1 in GBmal1KO animals, whereas this fraction was 90% ± 3% in WT females (Figure 4, A and B). Although Tom$^+$ neurons were found at various brain sites in GBmal1KO mice that additionally carried the tomato reporter allele, they were all BMAL1-positive, suggesting that recombination of the floxed *Bmal1* locus was ineffective in these cells (not shown), reminiscent of SCN neurons, in which the floxed *Bmal1* allele is also inefficiently recombined (31). Next, we ex-

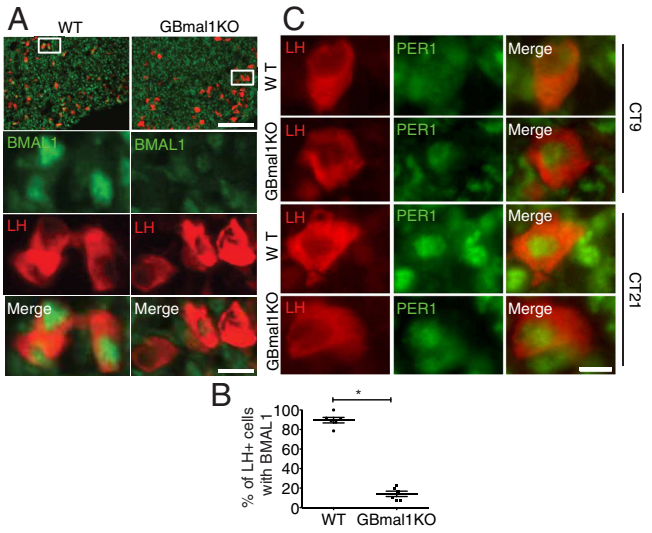

Figure 4. Loss of BMAL1 and molecular rhythms in GBmal1KO gonadotrope cells. A, Double immunolabeling for BMAL1 and LH of anterior pituitary sections from WT and GBmal1KO females. Boxed areas are shown enlarged underneath. B, Quantification of the fraction of LH cells that immunoreacted with BMAL1 antibodies; n = 6 for WT and GBmal1KO. By Student's *t* test: *, $P < .0001$. C, Immunostaining for PER1 and LH of anterior pituitary from WT and GBmal1KO females at CT 9 and 21. In WT gonadotropes, PER1 staining is predominantly cytoplasmic at CT 9, whereas it is largely nuclear at CT 21. GBmal1KO gonadotropes did not exhibit a time-of-day dependence in PER1 subcellular localization. PER1 staining was mainly nuclear at both time points, albeit more intense at CT21. Scale bars, 100 μm (A, top row), 20 μm (A), and 7 μm (C).

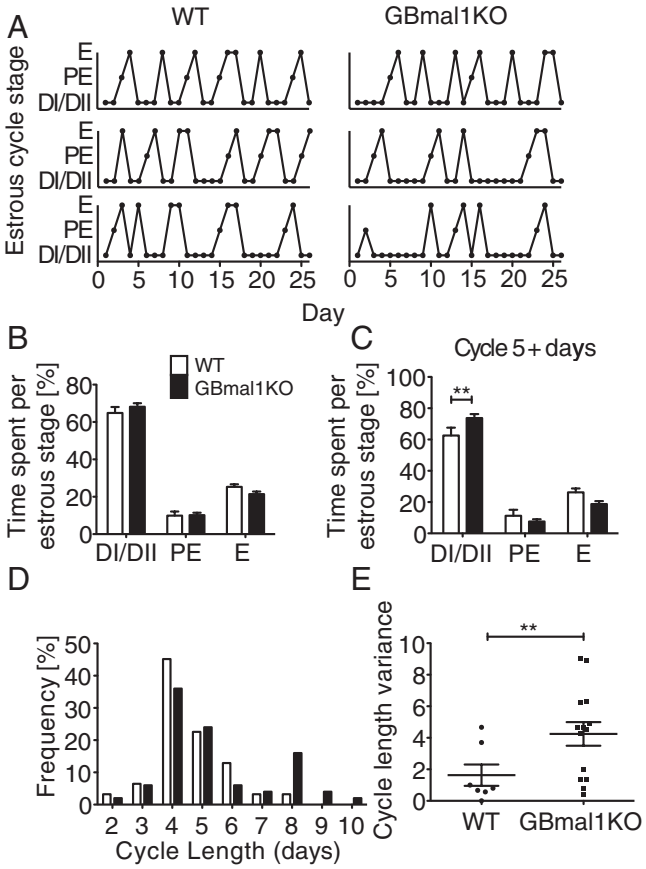

Figure 5. GBmal1KO estrous cycle characteristics. A, Estrous cycling in representative WT and GBmal1KO females. B, Proportion of time spent per estrous stage. C, Time spent per estrous stage during cycles with a length >5 days. By ANOVA: **, $P < .03$. D, Cycle length distribution within groups. E, Mean cycle length variance. By Student's *t* test: **, $P < .03$. Shown are mean ± SEM; n = 7 for WT and n = 14 for GBmal1KO. Abbreviations: E, estrus; PE, proestrus.

plored the effect of *Bmal1* ablation on PER1 subcellular localization in gonadotropes (Figure 4C). At circadian time (CT) 9, WT gonadotropes exhibited PER1 staining predominantly in the cytoplasm, whereas at CT 21, PER1 was bright and restricted to the nucleus. In contrast, GBmal1KO gonadotropes did not show a time-of-day variation in PER1 localization. At both time points examined, PER1 staining was predominantly nuclear albeit more intense at CT 21. These findings demonstrate that GRIC-Cre is effective in disrupting *Bmal1* and thus clock function selectively in pituitary gonadotropes.

GBmal1KO females exhibit estrous cycle instability and increased gonadotropin levels

To determine whether *Bmal1* disruption in gonadotropes leads to estrous deficits, we examined vaginal cytology in GBmal1KO females (Figure 5A). The proportion of time spent in each estrous stage did not significantly differ from WT (Figure 5B), except for cycles that extended 5 days in which case GBmal1KO females spent more time in metestrus (DI)/II (Figure 5C). However, we found a significant increase in cycle length variance in GBmal1KO females compared with their WT littermates (Figure 5, D and E).

We next collected blood from tail vein for 5 to 7 consecutive days at ZT 11 to determine serum gonadotropin levels (Figure 6, A and B). Both WT and GBmal1KO mice exhibited LH surge levels on proestrus (Figure 6, A and D), indicating that LH surge activation per se is not impaired in GBmal1KO animals. However, closer examination of serum content revealed that LH levels were significantly higher at all cycle stages in GBmal1KO animals (Figure 6, C and D). The average overall serum LH baseline concentration calculated from DI, DII, and estrous values was 207 ± 41.1 pg/mL for GBmal1KO compared with 58.3 ± 16.6 pg/mL for WT (Figure 6C). Similarly, the average LH level at ZT 11 on proestrus was higher in GBmal1KO females (17.4 ± 2.6 ng/mL) compared with WT (7.5 ± 2.5 ng/mL) (Figure 6D). Due to this general offset, the fold change representing the proestrous LH surge-to-baseline ratio did not differ between genotypes (Figure 6E).

We also detected a gradual variation of FSH serum levels along the estrous cycle in both genotypes, with trough levels typically found at DI/DII and maximum val-

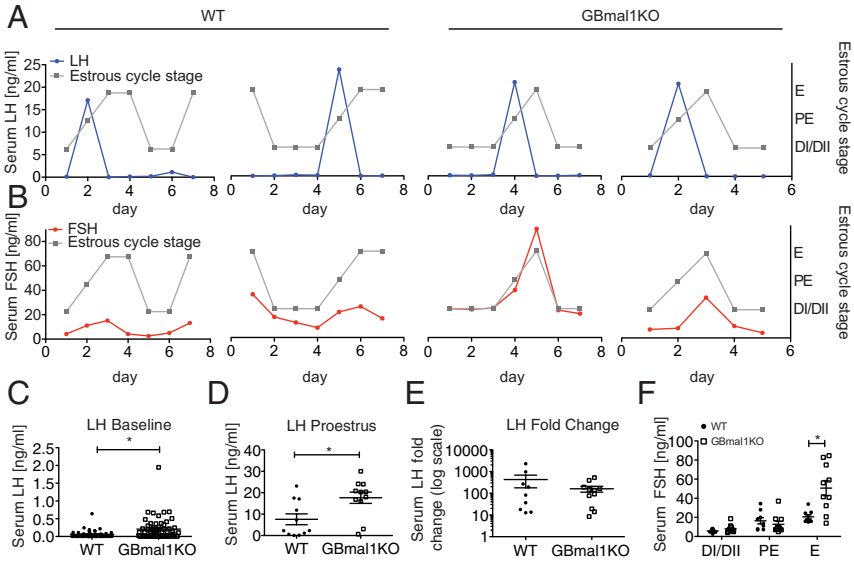

Figure 6. GBmal1KO gonadotropin profiling. A and B, Serum LH levels (A, blue trace) and FSH levels (B, red trace) measured daily at ZT 11 over 5 or 7 consecutive days in individual females. Gray traces indicate estrous stage. C, Baseline LH serum levels; dots indicate LH concentrations at individual, nonsurge time points. By Student's *t* test: *, $P < .003$. D, LH serum levels at ZT 11. By Student's *t* test: *, $P < .02$. E, Fold change of serum LH levels expressed as ratio of proestrus ZT11 level versus baseline minimum. F, FSH serum on DI/II, proestrus, and estrus day; in case of extended estrus, only the first day was considered.By ANOVA: *, $P < .0002$. Bars in dot plots indicate mean ± SEM; n = 9 (WT) and n = 11 (GBmal1KO) for C–F. Abbreviations: E, estrus; PE, proestrus.

ues on the day of estrus day (Figure 6B). Although DI/II and proestrous FSH levels did not differ between genotypes, estrous FSH was considerably elevated in GBmal1KO females (Figure 6E), possibly indicating a dysregulation of the secondary FSH surge. Both LH and FSH are known to influence progesterone and E2 serum levels by regulating their ovarian production. FSH induces the expression of aromatase in follicular granulosa cells (42), where it acts as the rate-limiting enzyme in E2 biosynthesis. Preovulatory LH is thought to stimulate progesterone production by upregulating P450scc in granulosa cells (43). However, progesterone and E2 serum concentrations at ZT 11 on proestrus did not significantly differ between genotypes (Table 1), indicating that the observed increases in gonadotropin levels after gonadotrope-specific *Bmal1* deletion did not affect production or secretion of these sex hormones, at least not on the day of proestrus.

Table 1. Reproductive Assessment of WT and GBmal1KO Female Mice[a]

	WT	GBmal1KO	*P* Value
Puberty onset (postnatal day)[b]	31.7 ± 0.72	31 ± 0.32	.57
Body weight (postnatal day 35)[b]	14.7 ± 0.28	14.2 ± 0.22	>.05[c]
Sex steroids[d]			
Progesterone, pg/mL	80.0 ± 27.4	106.8 ± 24.4	.16
E2, pg/mL	55.2 ± 24.1	43.25 ± 294	.90
Reproductive performance[e]			
Day of copulation	1.8 ± 0.3	2.3 ± 0.24	.31
Gestation, days	19 ± 0	18.75 ± 0.13	.40
Litter size	7.3 ± 0.66	7.8 ± 0.42	.48

[a] *P* values were determined by Student's *t* test unless otherwise specified. Values are mean ± SEM.

[b] For puberty onset, n = 24 WT and 27 GBmal1KO mice; for body weight at postnatal day 35, n = 31 WT and 33 GBmal1KO mice.

[c] ANOVA *P* value is based on postnatal days 25 to 85.

[d] Sex steroid serum levels were measured at ZT 11 on proestrus. For serum progesterone, n = 7 WT and 14 GBmal1KO mice; for serum estradiol, n = 7 WT and 9 GBmal1KO mice.

[e] For day of copulation, n = 7 WT and 14 GBmal1KO mice; for gestation and litter size, n = 3 WT and 12 GBmal1KO mice.

Because body-wide *Bmal1* knock out females display delayed puberty onset and infertility (16, 37), we investigated whether this is, at least in part, due to the loss of *Bmal1* expression in gonadotropes. The average time of puberty onset was around postnatal day 31 in both GBmal1KO and WT animals (Table 1), and GBmal1KO females were fertile and produced viable offspring. There was no effect of genotype on time to impregnation, gestation time, or litter size (Table 1), which together suggests that GBmal1KO females are reproductively normal.

Discussion

Failure to generate a proestrous LH surge has been previously reported in *Clock*$^{\Delta 19/\Delta 19}$ mice (14). It was cautioned, however, that the catheter-based blood sampling method employed in the study may have compromised LH regulation, because some of the WT control females lacked surges as well (37). Our results using *Bmal1*$^{-/-}$ females and a less invasive blood sampling approach via the tail vein now seem to confirm that disruption of the positive limb of the core circadian feedback loop leads to loss of the proestrous LH surge. It is theoretically possible that the LH surge has escaped detection in *Bmal1*$^{-/-}$ females due to the limited blood sampling. However, if the LH surge had indeed shifted toward the early estrous (ZT 23–7) time span, which we did not sample, then one would expect a corresponding shift in the timing of ovulation, which did not occur. In fact, we found COCs in each of the

Bmal1$^{-/-}$ females that we inspected at ZT 21 to 22, which precedes the time interval in question. If the LH surge had shifted only slightly in *Bmal1*$^{-/-}$ females, at least some elevation at a flanking sampling time point would be expected, given that the tail of the WT ZT 11 surge can be frequently detected at ZT 15 (see Figure 3C). However, such a shift could have indeed escaped detection if it would have been accompanied by a narrowing of the surge profile and/or a reduction in surge amplitude.

Despite this evident lack of an LH surge, *Bmal1*$^{-/-}$ females show estrous cycling and are able to ovulate, a result challenging the widely held view that the proestrous LH surge is an obligatory prerequisite for ovulation. Although a surge might be dispensable, our data do not preclude a requirement of LH per se for the ovulatory process. Notably, even though proestrous LH serum concentrations of *Bmal1*$^{-/-}$ mice were 50- to 100-fold lower than WT LH-surge levels, there was a trend toward slightly higher LH abundance at ZT 11 in *Bmal1*$^{-/-}$ females (Figure 3E). Given that oocytes are found at roughly the expected time and place within the oviducts on the day of estrus, it is possible that this slight proestrous elevation of LH provides a sufficient timing signal to trigger ovulation. Alternatively, ovulation in *Bmal1*$^{-/-}$ females might be elicited by other neurohumoral pathways that do not involve LH/FSH or by autonomous nervous system signaling. It seems unlikely, however, that ovulation in *Bmal1*$^{-/-}$ females can be triggered by ovarian signaling pathways alone, given that barbiturate treatment on the day of proestrus is capable of blocking not only the LH surge but also ovulation (1). Interestingly, there is evidence that regulation of both serum cortisol levels and adrenal clock phasing relies in part on direct neural input to the adrenal gland (45, 46). Serum cortisol oscillations were reported to persist in the absence of a rhythmic ACTH signal, suggesting that the thoracic splanchnic nerve, which innervates the adrenals, is able to transmit a 24-hour signal from the SCN (45, 47, 48). This view is further supported by the finding that behaviorally split hamsters show lateralization of clock gene rhythms in the paired adrenal structure; ie, there is a distinct and stable phase relationship between the clocks in the right and left adrenal glands and in the right and left SCN hemispheres that can be plausibly explained only by non-humoral–based entrainment (47). Interestingly, there are hints that a similar neurohumoral pathway dichotomy may exist in the context of ovulation; in rats, severing the superior ovarian nerve, which provides sympathetic input to the ovary, diminishes the number of oocytes shed on estrus (49–51) and ovarian noradrenalin levels rise concurrently with LH on proestrus (52). Furthermore, it was recently reported that heterotopically transplanted ovarian tissues encapsulated in dialysis membranes to prevent renervation by host nerves did not show signs of ovulation, whereas nonencapsulated ovarian transplants did (53). These results are consistent with the notion that sympathetic innervation plays an important role in the ovulatory process, which could explain why the elimination of the proestrous LH and FSH surge by disrupting *Bmal1* is not sufficient to prevent ovulation.

Bmal1$^{-/-}$ mice lack the increase in serum FSH on proestrus, suggesting that both the LH surge and the primary FSH surge require an intact circadian timing system. These data are in line with previous results demonstrating suppression of the primary FSH surge by GnRH-antagonist treatment on proestrus noon in OVX-E2 rats (54) and a time-of-day dependency of GnRH neuronal activation in OVX+E2 hamsters (55). The primary FSH surge is thought to induce cumulus expansion during the ovulatory process (56). However, visual inspection of the COCs accumulation in the fallopian ampullae on estrus did not reveal a decrease in the size or obvious morphological change of the cumulus matrix surrounding the ova, suggesting that the lack of the primary FSH surge in *Bmal1*$^{-/-}$ females did not overtly affect cumulus expansion.

We show that estrous cycling continues when *Bmal1*$^{-/-}$ mice are transferred to DD, an observation that has also been made in *Clock*$^{\Delta 19/\Delta 19}$ and *Vipr2*$^{-/-}$ females (57). However, although *Clock*$^{\Delta 19/\Delta 19}$ and *Vipr2*$^{-/-}$ mice typically exhibit rhythmic locomotor behavior for several days or even weeks in DD, *Bmal1*$^{-/-}$ mice are instantaneously arrhythmic when moved to DD, demonstrating a complete lack of endogenous circadian rhythm generation capacity in *Bmal1*$^{-/-}$ animals. Yet, estrous cycling continues in *Bmal1*$^{-/-}$ females, suggesting that it is governed by a self-sustaining infradian oscillatory process that does not require a 24-hour signal for its function. The estrous oscillator may, however, react on daily cues provided by the circadian clock and/or light to entrain their period to exact multiples of 24 hours, thus ensuring that each estrous stage is stably and appropriately aligned with the solar day. Interestingly, and in contrast to these findings, the sperm maturation cycle exhibits a period length that is generally not a multiple of 24 hours, and experiments with hamsters exposed to non–24-hour days indicate that spermatogenesis is not influenced by the circadian timing system or the light-dark cycle (58).

Given the complete loss of LH and primary FSH surge production in *Bmal1*$^{-/-}$ females, it appears plausible that the intrinsic clock in gonadotropes takes part in the regulation or generation of these surges. Surprisingly, however, extensive disruption of *Bmal1* within the gonadotrope population affected neither amplitude nor timing of the LH and primary FSH surges. *Bmal1* ablation led to

only a modest increase of baseline serum LH levels across all estrous cycle stages and a proportionate increase in LH surge levels. If we assume that the local gonadotrope clock contributes to reproduction by gating or partly driving the LH surge, then gonadotrope-specific *Bmal1* disruption would be expected to result in an alteration of amplitude or phase or a general degradation of the 24-hour LH profile. However, we detected only a slight general offset of the estrous cycle LH profile in GBmal1KO females; ie, surge and baseline levels were increased without a change in surge amplitude, which is difficult to reconcile with a circadian role for gonadotrope BMAL1 in LH regulation. It should be noted that because we sampled only at ZT 11 on proestrus, we cannot rule out that *Bmal1* ablation in gonadotropes results in an altered proestrous LH profile in addition to the observed elevation at ZT 11.

The detected increase in estrous cycle length variability in GBmal1KO females may reflect destabilization of the estrous process. Although LH and FSH serum levels seem only mildly dysregulated in GBmal1KO females when compared with $Bmal1^{-/-}$ and $Clock^{\Delta 19/\Delta 19}$, it is nevertheless tempting to speculate that the estrous impairments seen in all 3 genotypes are based, at least to some extent, on gonadotropin dysregulation.

There is also evidence that local clock function in the ovary contributes to reproductive performance. A time-of-day dependency of the ovulatory response to LH has been recently revealed in rats, suggesting that local ovarian clocks may gate LH receptor signaling (59). Although the SCN with its vasopressin- and vasoactive intestinal peptide-expressing neuronal populations seems to play a crucial role in LH surge control (60–62), it is plausible that clocks within the neural elements of the reproductive axis, such as GnRH and kisspeptin neurons, also contribute (30, 44, 55). Future research aimed at systematically manipulating clock function in individual cell types and tissues along the hypothalamic-pituitary-gonadal axis will likely be key for a comprehensive understanding of the circadian influence on reproduction.

Acknowledgments

We thank Chuck J. Weitz for the floxed *Bmal1* and *Bmal1-Luc* mice, Aude Villemain for expert technical assistance, and Sarah Robbins for critical reading of the manuscript.

Address all correspondence and requests for reprints to: Kai-Florian Storch, Douglas Mental Health University Institute, Department of Psychiatry, McGill University, 6875 LaSalle Boulevard, Montreal, Quebec H4H 1R3, Canada. E-mail: florian.storch@mcgill.ca.

This work was supported by Grant MOP-E-201759 of the Canadian Institutes of Health Research (CIHR) (to K.-F.S.); K.-F.S. holds a New Investigator Award from CIHR. H.O. is an Emmy Noether fellow of the German Research Foundation (DFG) and a Lichtenberg Fellow of the Volkswagen Foundation.

Disclosure Summary: The authors of this manuscript have nothing to disclose.

References

1. **Everett JW, Sawyer CH.** A 24-hour periodicity in the "LH-release apparatus" of female rats, disclosed by barbiturate sedation. *Endocrinology*. 1950;47:198–218.
2. **Legan SJ, Coon GA, Karsch FJ.** Role of estrogen as initiator of daily LH surges in the ovariectomized rat. *Endocrinology*. 1975;96:50–56.
3. **Christian CA, Mobley JL, Moenter SM.** Diurnal and estradiol-dependent changes in gonadotropin-releasing hormone neuron firing activity. *Proc Natl Acad Sci U S A*. 2005;102:15682–15687.
4. **Lucas RJ, Stirland JA, Darrow JM, Menaker M, Loudon AS.** Free running circadian rhythms of melatonin, luteinizing hormone, and cortisol in Syrian hamsters bearing the circadian tau mutation. *Endocrinology*. 1999;140:758–764.
5. **Dibner C, Schibler U, Albrecht U.** The mammalian circadian timing system: organization and coordination of central and peripheral clocks. *Annu Rev Physiol*. 2010;72:517–549.
6. **Kalsbeek A, Palm IF, La Fleur SE, et al.** SCN outputs and the hypothalamic balance of life. *J Biol Rhythms*. 2006;21:458–469.
7. **Mohawk JA, Green CB, Takahashi JS.** Central and peripheral circadian clocks in mammals. *Annu Rev Neurosci*. 2012;35:445–462.
8. **Gray GD, Söderstein P, Tallentire D, Davidson JM.** Effects of lesions in various structures of suprachiasmatic-preoptic region on LH regulation and sexual behavior in female rats. *Neuroendocrinology*. 1978;25:174–191.
9. **Stephan FK, Zucker I.** Circadian rhythms in drinking behavior and locomotor activity of rats are eliminated by hypothalamic lesions. *Proc Natl Acad Sci U S A*. 1972;69:1583–1586.
10. **Wiegand SJ, Terasawa E.** Discrete lesions reveal functional heterogeneity of suprachiasmatic structures in regulation of gonadotropin secretion in the female rat. *Neuroendocrinology*. 1982;34:395–404.
11. **de la Iglesia HO, Meyer J, Carpino A Jr, Schwartz WJ.** Antiphase oscillation of the left and right suprachiasmatic nuclei. *Science*. 2000;290:799–801.
12. **de la Iglesia HO, Meyer J, Schwartz WJ.** Lateralization of circadian pacemaker output: Activation of left- and right-sided luteinizing hormone-releasing hormone neurons involves a neural rather than a humoral pathway. *J Neurosci*. 2003;23:7412–7414.
13. **Vitaterna MH, King DP, Chang AM, et al.** Mutagenesis and mapping of a mouse gene, Clock, essential for circadian behavior. *Science*. 1994;264:719–725.
14. **Miller BH, Olson SL, Turek FW, Levine JE, Horton TH, Takahashi JS.** Circadian clock mutation disrupts estrous cyclicity and maintenance of pregnancy. *Curr Biol*. 2004;14:1367–1373.
15. **Kennaway DJ, Boden MJ, Voultsios A.** Reproductive performance in female Clock Delta19 mutant mice. *Reprod Fertil Dev*. 2004;16:801–810.
16. **Ratajczak CK, Boehle KL, Muglia LJ.** Impaired steroidogenesis and implantation failure in $Bmal1^{-/-}$ mice. *Endocrinology*. 2009;150:1879–1885.
17. **Bunger MK, Wilsbacher LD, Moran SM, et al.** Mop3 is an essential component of the master circadian pacemaker in mammals. *Cell*. 2000;103:1009–1017.

18. **Nakamura TJ, Sellix MT, Kudo T, et al.** Influence of the estrous cycle on clock gene expression in reproductive tissues: effects of fluctuating ovarian steroid hormone levels. *Steroids*. 2010;75:203–212.
19. **Guillaumond F, Becquet D, Boyer B, et al.** DNA microarray analysis and functional profile of pituitary transcriptome under core-clock protein BMAL1 control. *Chronobiol Int*. 2012;29:103–130.
20. **Naor Z.** Signaling by G-protein-coupled receptor (GPCR): studies on the GnRH receptor. *Front Neuroendocrinol*. 2009;30:10–29.
21. **Pawson AJ, McNeilly AS.** The pituitary effects of GnRH. *Anim Reprod Sci*. 2005;88:75–94.
22. **Bur IM, Zouaoui S, Fontanaud P, et al.** The comparison between circadian oscillators in mouse liver and pituitary gland reveals different integration of feeding and light schedules. *PLoS ONE*. 2010;5:e15316.
23. **Yoo SH, Yamazaki S, Lowrey PL, et al.** PERIOD2::LUCIFERASE real-time reporting of circadian dynamics reveals persistent circadian oscillations in mouse peripheral tissues. *Proc Natl Acad Sci U S A*. 2004;101:5339–5346.
24. **Resuehr HE, Resuehr D, Olcese J.** Induction of mPer1 expression by GnRH in pituitary gonadotrope cells involves EGR-1. *Mol Cell Endocrinol*. 2009;311:120–125.
25. **Resuehr D, Wildemann U, Sikes H, Olcese J.** E-box regulation of gonadotropin-releasing hormone (GnRH) receptor expression in immortalized gonadotrope cells. *Mol Cell Endocrinol*. 2007;278:36–43.
26. **Robles MS, Boyault C, Knutti D, Padmanabhan K, Weitz CJ.** Identification of RACK1 and protein kinase Calpha as integral components of the mammalian circadian clock. *Science*. 2010;327:463–466.
27. **Sambrook J, Russell DW.** *The Condensed Protocols From Molecular Cloning: A Laboratory Manual*. Cold Spring Harbor, NY: Cold Spring Harbor Laboratory Press; 2006.
28. **Fahrenkrug J, Georg B, Hannibal J, Hindersson P, Gräs S.** Diurnal rhythmicity of the clock genes Per1 and Per2 in the rat ovary. *Endocrinology*. 2006;147:3769–3776.
29. **Yamazaki S, Takahashi JS.** Real-time luminescence reporting of circadian gene expression in mammals. *Methods Enzymol*. 2005;393:288–301.
30. **Chappell PE, White RS, Mellon PL.** Circadian gene expression regulates pulsatile gonadotropin-releasing hormone (GnRH) secretory patterns in the hypothalamic GnRH-secreting GT1–7 cell line. *J Neurosci*. 2003;23:11202–11213.
31. **Husse J, Zhou X, Shostak A, Oster H, Eichele G.** Synaptotagmin10-Cre, a driver to disrupt clock genes in the SCN. *J Biol Rhythms*. 2011;26:379–389.
32. **Arai KY, Ohshima K, Watanabe G, Arai K, Uehara K, Taya K.** Dynamics of messenger RNAs encoding inhibin/activin subunits and follistatin in the ovary during the rat estrous cycle. *Biol Reprod*. 2002;66:1119–1126.
33. **Woodruff TK, Besecke LM, Groome N, Draper LB, Schwartz NB, Weiss J.** Inhibin A and inhibin B are inversely correlated to follicle-stimulating hormone, yet are discordant during the follicular phase of the rat estrous cycle, and inhibin A is expressed in a sexually dimorphic manner. *Endocrinology*. 1996;137:5463–5467.
34. **Schwartz NB, Channing CP.** Evidence for ovarian "inhibin": suppression of the secondary rise in serum follicle stimulating hormone levels in proestrous rats by injection of porcine follicular fluid. *Proc Natl Acad Sci U S A*. 1977;74:5721–5724.
35. **Jochle W.** Current research in coitus-induced ovulation: a review. *J Reprod Fertil Suppl*. 1975;165–207.
36. **Ishikawa H, Endo A.** Prolongation of duration of ovulation in ageing mice. *J Reprod Fertil*. 1996;108:167–170.
37. **Boden MJ, Varcoe TJ, Voultsios A, Kennaway DJ.** Reproductive biology of female Bmal1 null mice. *Reproduction*. 2010;139:1077–1090.
38. **Wen S, Schwarz JR, Niculescu D, et al.** Functional characterization of genetically labeled gonadotropes. *Endocrinology*. 2008;149:2701–2711.
39. **Madisen L, Zwingman TA, Sunkin SM, et al.** A robust and high-throughput Cre reporting and characterization system for the whole mouse brain. *Nat Neurosci*. 2010;13:U133–U311.
40. **Wen S, Götze IN, Mai O, Schauer C, Leinders-Zufall T, Boehm U.** Genetic identification of GnRH receptor neurons: a new model for studying neural circuits underlying reproductive physiology in the mouse brain. *Endocrinology*. 2011;152:1515–1526.
41. **Storch KF, Paz C, Signorovitch J, Raviola E, Pawlyk B, Li T, Weitz CJ.** Intrinsic circadian clock of the mammalian retina: importance for retinal processing of visual information. *Cell*. 2007;130:730–741.
42. **Fitzpatrick SL, Richards JS.** Regulation of cytochrome P450 aromatase messenger ribonucleic acid and activity by steroids and gonadotropins in rat granulosa cells. *Endocrinology*. 1991;129:1452–1462.
43. **Chaffin CL, Stouffer RL.** Local role of progesterone in the ovary during the periovulatory interval. *Rev Endocr Metab Disord*. 2002;3:65–72.
44. **Robertson JL, Clifton DK, de la Iglesia HO, Steiner RA, Kauffman AS.** Circadian regulation of Kiss1 neurons: implications for timing the preovulatory gonadotropin-releasing hormone/luteinizing hormone surge. *Endocrinology*. 2009;150:3664–3671.
45. **Lilley TR, Wotus C, Taylor D, Lee JM, de la Iglesia HO.** Circadian regulation of cortisol release in behaviorally split golden hamsters. *Endocrinology*. 2012;153:732–738.
46. **Vujovic N, Davidson AJ, Menaker M.** Sympathetic input modulates, but does not determine, phase of peripheral circadian oscillators. *Am J Physiol Regul Integr Comp Physiol*. 2008;295:R355–R360.
47. **Mahoney CE, Brewer D, Costello MK, Brewer JM, Bittman EL.** Lateralization of the central circadian pacemaker output: a test of neural control of peripheral oscillator phase. *Am J Physiol Regul Integr Comp Physiol*. 2010;299:R751–R761.
48. **Ishida A, Mutoh T, Ueyama T, et al.** Light activates the adrenal gland: timing of gene expression and glucocorticoid release. *Cell Metab*. 2005;2:297–307.
49. **Chávez R, Carrizosa L, Domínguez R, Zipitría D** Effects of superior ovarian nerve section on spontaneous and induced ovulation in the adult rat. *Med Sci Res*. 1991;19:41–42.
50. **Domínguez R, Zipitría D.** Longterm effects of guanethidine administration on the ovulatory response of the rat. *IRCS Med Sci*. 1980;8:352.
51. **Flores A, Ayala ME, Domínguez R.** Does noradrenergic peripheral innervation have a different role in the regulation of ovulation in the pubertal and the adult rat. *Med Sci Res*. 1990;18:817–818.
52. **Wolf R, Meier-Fleitmann A, Düker EM, Wuttke W.** Intraovarian secretion of catecholamines, oxytocin, β-endorphin, and γ-aminobutyric-acid in freely moving rats: development of a push-pull tubing method. *Biol Reprod*. 1986;35:599–607.
53. **Yoshikawa T, Sellix M, Pezuk P, Menaker M.** Timing of the ovarian circadian clock is regulated by gonadotropins. *Endocrinology*. 2009;150:4338–4347.
54. **Schwartz NB, Rivier C, Rivier J, Vale WW.** Effect of gonadotropin-releasing hormone antagonists on serum follicle-stimulating hormone and luteinizing hormone under conditions of singular follicle-stimulating hormone secretion. *Biol Reprod*. 1985;32:391–398.
55. **Williams WP 3rd, Jarjisian SG, Mikkelsen JD, Kriegsfeld LJ.** Circadian control of kisspeptin and a gated GnRH response mediate the preovulatory luteinizing hormone surge. *Endocrinology*. 2011;152:595–606.
56. **Eppig JJ.** FSH stimulates hyaluronic acid synthesis by oocyte-cumulus cell complexes from mouse preovulatory follicles. *Nature*. 1979;281:483–484.

57. **Dolatshad H, Campbell EA, O'Hara L, Maywood ES, Hastings MH, Johnson MH.** Developmental and reproductive performance in circadian mutant mice. *Hum Reprod*. 2006;21:68–79.
58. **Klose M, Grote K, Lerchl A.** Temporal Control of Spermatogenesis Is Independent of the Central Circadian Pacemaker in Djungarian Hamsters (Phodopus sungorus). *Biol Reprod*. 2011;84:124–129.
59. **Sellix MT, Yoshikawa T, Menaker M.** A circadian egg timer gates ovulation. *Curr Biol*. 2010;20:R266–R267.
60. **Christian CA, Moenter SM.** Vasoactive intestinal polypeptide can excite gonadotropin-releasing hormone neurons in a manner dependent on estradiol and gated by time of day. *Endocrinology*. 2008;149:3130–3136.
61. **Miller BH, Olson SL, Levine JE, Turek FW, Horton TH, Takahashi JS.** Vasopressin regulation of the proestrous luteinizing hormone surge in wild-type and Clock mutant mice. *Biol Reprod*. 2006;75:778–784.
62. **Smarr BL, Morris E, de la Iglesia HO.** The dorsomedial suprachiasmatic nucleus times circadian expression of Kiss1 and the luteinizing hormone surge. *Endocrinology*. 2012;153:2839–2850.